Cancer Chemother Pharmacol (1986) 16: 211–217

Cancer Chemotherapy and Pharmacology

Cellular pharmacology and antitumor activity of *N*-(*p*-azidobenzoyl)-daunorubicin, a photoactive anthracycline analogue

Steven D. Averbuch, Ronald E. Clawson*, Nicholas R. Bachur and Ronald L. Felsted

Laboratory of Biological Chemistry, Developmental Therapeutics Program, Division of Cancer Treatment, National Cancer Institute, National Institutes of Health, Building 37, Room 5D02 Bethesda, MD 20205, USA

Summary. We have previously utilized *N*-(*p*-azidobenzoyl)daunorubicin (NABD), a photoactive analogue of daunorubicin (DNR), to identify unique anthracycline-binding polypeptides in rodent tissues and in tumor cells. Using cultured P388 tumor cells, we have now compared the cellular pharmacology and antitumor activity of NABD with that of DNR. Although rapidly accumulated by cells, the intracellular concentration of NABD was less than 20% that of DNR at steady-state levels. The cellular uptake of both drugs by P388 cells was dependent on extracellular drug concentration in the medium and on temperature. The rapid efflux of NABD and DNR from P388 cells in drug-free medium was reduced at lowered temperature (0 °C). Cytofluorescence microscopy demonstrated that NABD was predominantly localized in the cytoplasm, in contrast to the nuclear localization of DNR. NABD produced dose-dependent inhibition of [^{3}H]thymidine (IC_{50} = 10.0 μ*M*) and [^{3}H]uridine (IC_{50} = 1.60 μ*M*) incorporation in P388 cells to a lesser degree than DNR ([^{3}H]thymidine, IC_{50} = 0.15 μ*M* and [^{3}H]uridine, IC_{50} = 0.70 μ*M*). Continuous exposure to NABD inhibited P388 cell proliferation with an IC_{50} of 0.27 μ*M*, compared with an IC_{50} of 0.017 μ*M* for DNR. NABD is a pharmacologically active, photoactive analogue of DNR, which possesses properties different from those of the parent drug but similar to those of other anthracycline analogues. Photoaffinity labeling studies with NABD may identify important cytoplasmic constitutents which interact with this type of anthracycline and perhaps with the anthracycline antibiotics in general.

Introduction

The anthracycline antibiotics represent an important class of antineoplastic drugs, which are cytostatic and cytotoxic to a broad spectrum of tumors [1, 3, 12, 24, 27]. Studies of anthracyclines in experimental biological systems have shown these compounds to interact with multiple cellular organelles and macromolecules [4–8, 10–12, 18, 19, 22, 23, 25, 30]. However, in most instances the identification of specific macromolecular targets for drug interaction is confounded by the presence of a high degree of nonspecific adsorption of the anthracyclines to biological material and experimental apparatus.

Photoaffinity labeling is an experimental approach which can circumvent these limitations [9, 15]. To characterize anthracycline interactions with specific cellular macromolecules we have recently utilized a photoactive anthracycline analogue, *N*-(*p*-azidobenzoyl)daunorubicin (NABD), to identify unique anthracycline-binding polypeptides in rodent tissues [11, 18; R. L. Felsted et al., 1985, submitted for publication] and in tumor cells [4, 5]. The preparation of this photoactive analogue necessitated a chemical modification of the daunosamine sugar, which may significantly change the chemical and pharmacological properties of the analogue in comparison with the parent drug. We therefore studied the cellular pharmacology and antitumor activity of the photoactive analogue, NABD, compared with daunorubicin (DNR), to clarify the relationship between photoaffinity-labeled anthracycline targets and anthracycline antibiotic mechanism of action.

Materials and methods

Cell lines. P388 murine leukemia cells were maintained in vitro by serial culture in RPMI Medium 1640 (M. A. Bioproducts, Whittaker Corporation, Walkersville, Md) containing penicillin 50 units/ml, streptomycin 50 μg/ml *L*-glutamine 2 μmol/ml (Flow Laboratories Inc., Rockville, Md), β-mercaptoethanol 10 μ*M* (Sigma Chemical Company, St. Louis, Mo), and 10% fetal bovine serum (FBS) (Flow Laboratories Inc.) at 37 °C in 5% CO_2 atmosphere. Under these conditions, cells had a population-doubling time of 14–16 h and achieved a maximum cell density of $1.8–2.2 \times 10^6$ cells/ml. Except where noted, all experiments were performed with the medium described above. Cell density was determined with the aid of a Coulter counter (Coulter Electronics Inc., Hialeah, Fla).

* *Present address:* Medical Chemical Defense R and D Program, U. S. Army Medical R and D Command, Att. 5GRDPLE, Fort Detrick, Frederick, MD 21701, USA

Offprint requests to: S. D. Averbuch, Clinical Pharmacology Branch, DCT, NCI, National Institutes of Health, Building 10, Room 6N119, Bethesda, MD 20205, USA

Abbreviations used: NABD, *N*-(*p*-azidobenzoyl)daunorubicin; DNR, daunorubicin; D_2, daunorubicinol; $NABD_2$, *N*-(*p*-azidobenzoyl)daunorubicinol; dDa, 7-deoxydaunorubicin aglycone; dD_{2a}, 7-deoxydaunorubicinol aglycone; TLC, thin-layer chromatography; HPLC, high-pressure liquid chromatography; THF, tetrahydrofuran; PBS, phosphate-buffered saline; DMSO, dimethylsulfoxide

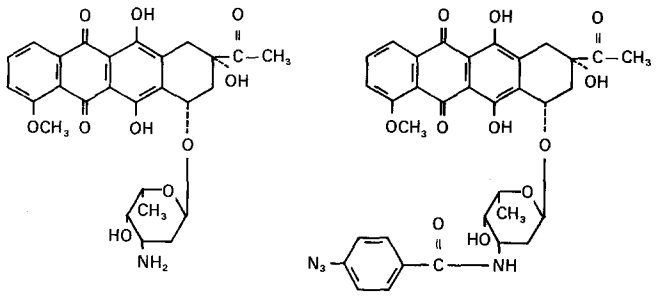

Fig. 1. Structures of daunorubicin (DNR) and *N*-(*p*-azidobenzoyl)daunorubicin (NABD)

Isolation of human neutrophils. Neutrophils were isolated by a Ficoll-Hypaque gradient as previously described [14].

Drugs. Daunorubicin (DNR, NSC 82151, Fig. 1) was obtained from the Developmental Therapeutics Program, National Cancer Institute, Bethesda, Md.

N-(*p*-Azidobenzoyl)daunorubicin (NABD, NSC 372108, Fig. 1) was prepared by *N*-azidobenzoylation of daunorubicin with *N*-hydroxysuccinimidyl-4-azidobenzoate (Pierce Chemical Co., Rockford, Ill). The synthesis and characterization of the final product, NABD, has been described elsewhere (R. L. Felsted et al., 1985, submitted for publication). NABD photoactivation occurs following exposure to intense, low-wavelength (<350 nm) light and therefore all drug experiments described here were performed in ambient light. Partition coefficients were determined according to the method of Kessel [20], and the ratios of drug concentration in the octanol:aqueous phase were 1.68 and >119 for DNR and NABD, respectively. Daunorubicinol (D_2) and *N*-(*p*-azidobenzoyl) daunorubicinol ($NABD_2$) were prepared enzymatically from DNR and NABD, respectively, with 0.138 mg/ml rat liver daunorubicin reductase in 5 m*M* NADPH (P and L Biochemicals, Milwaukee, Wis) and 10 m*M* Tris-HCl buffer, pH 8.5 [16]. 7-Deoxydaunorubicin aglycone (dDa) and 7-deoxydaunorubinicol aglycone (dD_{2a}) were prepared as described by Smith et al. [26].

Fluorescence spectra. Fluorescence excitation and emission spectra were obtained with a Model SPF-500 absolute spectrophotometer (American Instrument Co., Silver Spring, Md). DNR and NABD had identical activation maxima at 470 nm and emission maxima at 585 nm.

TLC and HPLC methods. Silica gel thin-layer chromatography (TLC) was performed as described previously [28]. In a solvent system containing chloroform: methanol: acetic acid (100:2:2.5), NABD appeared as a single fluorescent spot with an R_f value of 0.27, while DNR remained at the origin.

The high-pressure liquid chromatography (HPLC) system consisted of two Beckman 100A pumps fitted with a μBondapak phenyl column (3.9 mm × 30 cm, Waters Associates, Milford, Mass) and a Gilson 121 fluorometer containing activation and emission filters of 480 and 560 nm, respectively. The previously described [2] reversed-phase method of a 10-min gradient of 15%–50% tetrahydrofuran (THF) in 0.1 g/100 ml ammonium formate buffer, pH 4.0, at a flow rate of 2 ml/min was modified slightly by the addition of 5 min isocratic 50% THF in buffer at the end of the gradient. With this system, DNR, D_2, NABD, $NABD_2$, dDa, and dD_{2a} have retention times of 10.1, 8.6, 13.7, 12.5, 11.7, and 9.8 min, respectively.

Incubation conditions. Tumor cells in late log phase growth were washed twice with ice-cold phosphate-buffered saline (PBS) and resuspended in fresh medium. After preincubation of the cells for 60 min, the drugs were added in an equal volume of prewarmed (37 °C) medium so that the final cell density was 10^6/ml. Owing to the poor aqueous solubility of NABD, this drug was dissolved in dimethylsulfoxide (DMSO) to give a final DMSO concentration of 0.5% in medium. DNR was handled identically. Unless otherwise indicated, all incubations were performed at 37 °C in a metabolic shaking incubator.

Assay of drug uptake and metabolism. Following incubation, 1.0 ml cells was added to 0.4 ml F50 Versilube silicone fluid (General Electric Co., Waterford, NY) in 1.5-ml micro test tubes, and the cells were centrifuged at 13 000 *g* for 1 min. The supernatant solution was poured off and the sedimented cells were resuspended in 1.5 ml 0.54 *N* H_2SO_4 in 75% isopropanol. Fluorescence was determined with excitation at 470 nm and emission at 585 nm, and drug content was calculated by comparison with simultaneously performed DNR and NABD standards [19]. A duplicate sample of sedimented cells was resuspended in 1.0 ml medium and the cell density determined. In drug metabolism experiments, sedimented cells or medium were/was extracted with chloroform:methanol (2:1, v:v). The extracts were evaporated to dryness under a stream of nitrogen gas, redissolved in small volumes of methanol, and analyzed by TLC and HPLC. P388 cell-free homogenates were prepared by washing 10^7 cells twice with 10 ml ice-cold PBS, followed by resuspension and brief sonication in 50 m*M* potassium phosphate buffer (pH 7.4). The homogenate (200 μg protein) was incubated with 10 μ*M* DNR or NABD in a final volume of 0.1 ml 10 m*M* MOPS buffer, pH 7.0, containing 1% DMSO for 60 min. The incubations were terminated by the addition of 1.0 ml chloroform:methanol (2:1, v:v), clarified by centrifugation (13 000 *g*, 2 min), and the fluorescent metabolites present in the supernatant solution were analyzed by HPLC.

Efflux experiments. After incubation with 10 μ*M* DNR or NABD for 120 min, cells were sedimented, washed twice with 10 ml ice-cold PBS, and resuspended in drug-free medium at either 0 or 37 °C. After varying periods of incubation, cells were sedimented by centrifugation (13 000 *g*, 1 min) and their remaining drug content was determined fluorimetrically as described above.

Cytofluorescence microscopy. Cells incubated with DNR or NABD were washed once or twice with 0.154 *M* NaCl, and the sedimented cells were resuspended in a small volume of 0.154 *M* NaCl. Cell suspensions were examined immediately on an American Optical Model 10 microscope (American Optical Corp., Buffalo, NY) fitted with an HBO 50 mercury arc lamp and FITC interference filter for incident illumination and 500 nm and 515 nm secondary filters. Photomicrographs were made on Kodak Ektachrome film (ED 135, ASA 200).

Incorporation of radioactive macromolecular precursors. After incubation of cells for 120 min with NABD or DNR, 0.1 ml medium containing 1 μCi [methyl-^{3}H]thymidine (2.0 Ci/mmol, New England Nuclear, Boston, Mass), 1 μCi [^{3}H(G)]uridine (6.0 Ci/mmol, New England Nuclear) or 1 μCi [3,4-^{3}H]valine (65 Ci/mmol, New England Nuclear) was added to the cultures. After incubation for 60 min with radiolabeled nucleoside or 120 min with radiolabeled amino acid, cells were assayed for incorporation of ^{3}H into trichloroacetic acid-precipitable material as described previously [17].

Cell growth inhibition assay. After washing with ice-cold PBS, P388 cells (2×10^5/ml) were resuspended in fresh medium containing various concentrations of NABD or DNR in 0.5% DMSO for increasing times of exposure up to 72 h. Following an initial lag phase, cell growth in control and drug-treated samples was linear up to 72 h, at which time cell density was determined and the slope of the log cell density-vs-time plot was calculated. The growth rate at each drug concentration was expressed as a percentage of the control growth rate. Dose-response curves were generated and the drug concentration required to inhibit 50% of cell growth rate (IC_{50}) was determined from a logarithmic curve fit analysis.

Results

Drug accumulation by whole cells

At 37 °C, DNR was taken up rapidly by P388 cells over the first 20 min, followed by an accumulation which approached steady state by 60 min. NABD uptake was also initially rapid, but in contrast to DNR, steady state levels were achieved at 10 min and total drug accumulation was much less (Fig. 2). The cellular accumulation of DNR exceeded NABD accumulation by a factor of 5–6 at steady state. Assuming a mean cell size of approximately 800 μm^3 [29], this corresponds to a cell : medium molar ratio of 344 for DNR and 50 for NABD. The cellular uptake of both DNR and NABD were temperature-sensitive, cellular accumulation at 0 °C being much less than at 37 °C (Fig. 2). The uptake of both anthracyclines was concentration-dependent (Fig. 3); and for drug concentrations from 0.5 to 10 μ*M* the uptake of DNR was 5–10 times that of NABD.

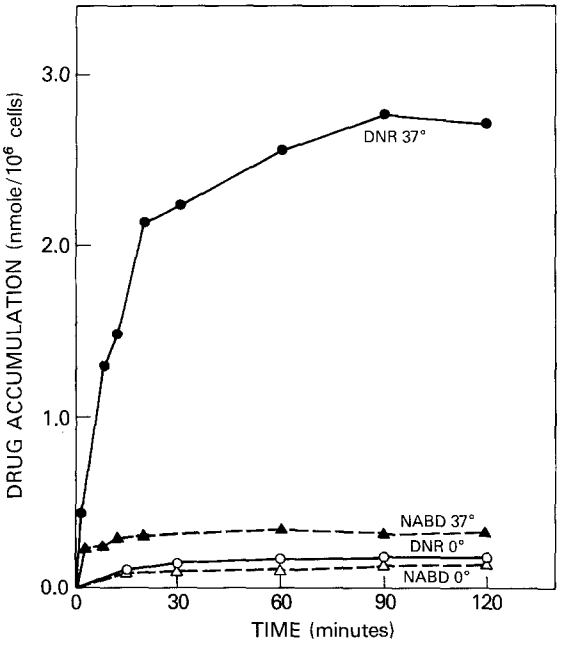

Fig. 2. Effect of temperature on the accumulation of DNR and NABD by P388 cells. *Points* each represent the mean of four experimental determinations. Each SD was < 24% of the mean

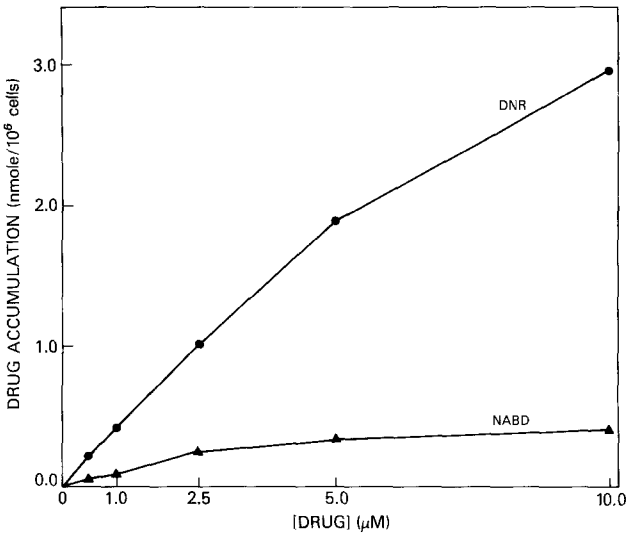

Fig. 3. Accumulation of DNR and NABD by P388 cells. *Points* represent the means of triplicate samples from three separate experiments. Each SD was < 22% of the mean

Drug efflux by whole cells

DNR had a rapid initial efflux, which slowed and approached a new steady state after 30 min (Fig. 4). NABD exited cells extremely rapidly, so that intracellular drug content was undetectable 5 min following resuspension in fresh medium (Fig. 4). At steady state cells retained over

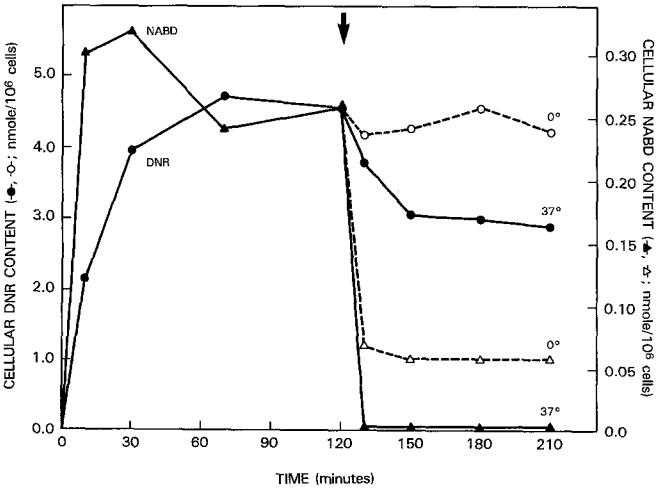

Fig. 4. Effect of temperature on the efflux of DNR or NABD from P388 cells. *Points* represent means of three experimental determinations. Each SD was < 19% of the mean

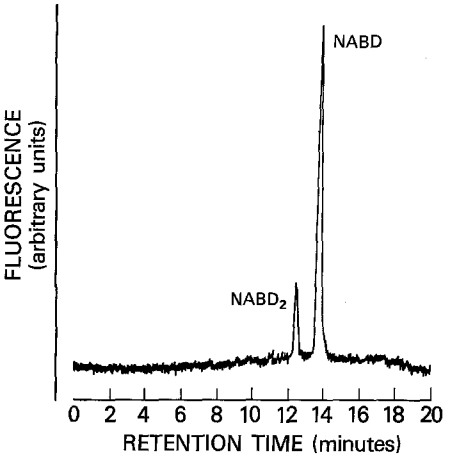

Fig. 5. Reverse-phase HPLC separation of a chloroform:methanol (2:1; v:v) extract of P388 cells (10^6/ml) after incubation with 10 μ*M* NABD for 2 h. At this time point, $NABD_2$ accounted for 15% of the total fluorescence as determined from the integrated area under the curve for each peak

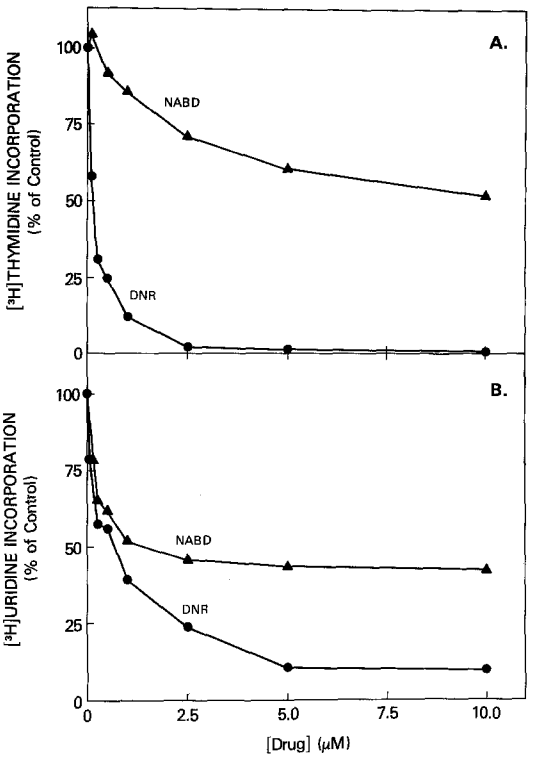

Fig. 7 (A, B). Effect of DNR and NABD on [^{3}H]thymidine and [^{3}H]uridine incorporation by P388 cells. Cells (10^6/ml) were incubated for 2 h with various concentrations of DNR or NABD and incorporation of [^{3}H]thymidine **(A)** or [^{3}H]uridine **(B)** into trichloroacetic acid-precipitable material was then assessed as described in *Materials and methods*. *Points* represent the means of triplicate samples from three separate experiments. Each SD was < 10% of the mean

60% of the accumulated DNR, whereas the NABD-treated cells were free of detectable drug.

The efflux of both drugs occurred by way of a process that was reduced at 0 °C compared with 37 °C. However, this temperature dependency was much greater for DNR egress, since the new steady-state drug level was not significantly different in drug-free medium, whereas NABD steady-state cellular content was reduced by over 70% at 0 °C (Fig. 4).

Drug metabolism by whole cells and cell homogenates

HPLC analysis of extracts from P388 or medium incubated with DNR or NABD for various times of incubation showed a time-dependent production of a fluorescent compound that cochromatographed with $NABD_2$ (Fig. 5). This compound is the product of the side chain C-13 carbonyl reduction to the more polar alcohol which is the major metabolite of class I anthracycline antibiotics [25]. By 72 h this NABD metabolite accounted for 60% of the total fluorescence extracted from the sedimented cells. The parent NABD accounted for 25%, and unknown metabolites accounted for 15%, of total fluorescence. An equal propor-

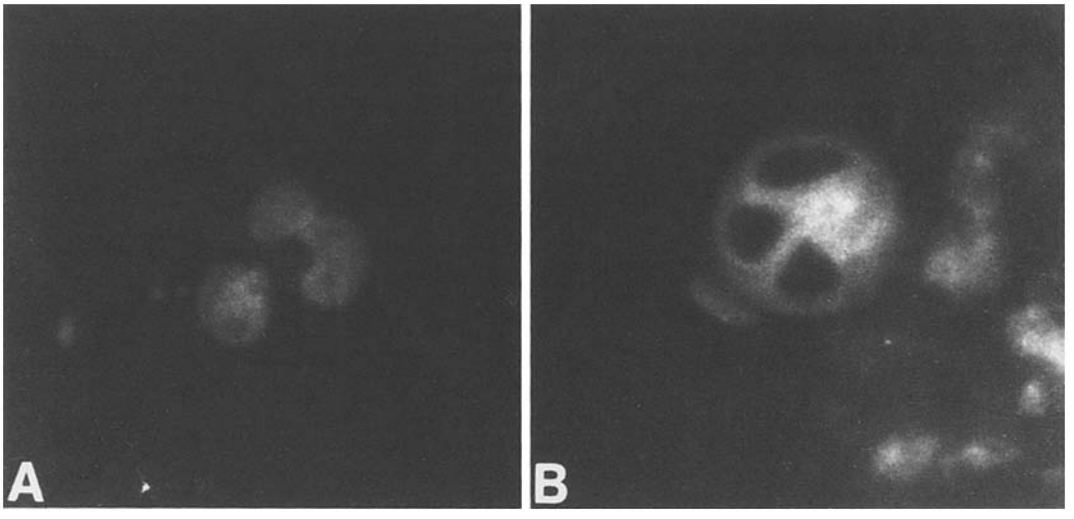

Fig. 6 (A, B). Cytofluorescence microscopy of human neutrophils incubated with DNR **(A)** or NABD **(B)**. Human neutrophils were isolated as described in *Materials and methods* and incubated with 20 μ*M* drug. After 15 min, cells were washed once with ice-cold 0.154 *M* NaCl and examined by fluorescent microscopy. (× 500)

Table 1. Effect of DNR and NABD on [^{3}H]thymidine and [^{3}H]uridine incorporation in P388 tumor cells

Drug	IC_{50} (μM)[a]				IC_{50} Ratio ([^{3}H]thymidine: [^{3}H]uridine)	
	[^{3}H]Thymidine		[^{3}H]Uridine			
	Extracellular	Intracellular	Extracellular	Intracellular	Extracellular	Intracellular
DNR	0.15[b]	100	0.70	375	0.21	0.27
NABD	10.0	500	1.60	200	6.25	2.50

[a] IC_{50}, 50% inhibitory concentration
[b] Mean of three triplicate experiments

tion of NABD and $NABD_2$ was present in the supernatant fraction at 72 h. When NABD was incubated in medium without cells no fluorescent metabolites were detected. When P388 cellular homogenate was incubated with NABD at 25 °C in the presence of air for 60 min no $NABD_2$ was formed. Under anaerobic conditions in the presence of excess 1 m*M* NADPH approximately 1% of NABD was converted to $NABD_2$ after 60 min at 37 °C. Neither the photolytic product, *N*-(*p*-aminobenzoyl)-DNR, nor DNR was formed in either whole cells or cell homogenates incubated with NABD.

Cytofluorescence microscopy

The intracellular distribution of DNR and NABD was evaluated by cytofluorescence microscopy. As described previously [14], DNR was concentrated in cell nuclei with slight cytoplasmic localization (Fig. 6). In contrast, NABD showed cytoplasmic accumulation, with little if any drug fluorescence observed in cell nuclei (Fig. 6). Although most easily seen in human neutrophils (Fig. 6), these characteristic intracellular drug localization patterns were also observed in P388 cells.

Inhibition of cellular macromolecular synthesis

As with DNR, NABD produced dose-dependent inhibition of [^{3}H]thymidine and [^{3}H]uridine incorporation in intact P388 cells (Fig. 7). However, NABD inhibited labeled precursor incorporation to a lesser degree than DNR (Table 1). In addition, no more than 50% inhibition was observed following a 2-h exposure of cells to NABD, in spite of high concentrations of the drug. In contrast to DNR, NABD inhibited [^{3}H]uridine incorporation more effectively than [^{3}H]thymidine incorporation (Table 1). NABD had no effect on protein synthesis as determined by [^{3}H]valine incorporation.

Cell growth inhibition in vitro

Following continuous exposure to NABD, P388 cell growth was inhibited in a dose-dependent fashion, with an IC_{50} of 0.27 μ*M* as against an IC_{50} of 0.017 μ*M* for DNR. The difference in cell growth IC_{50} between DNR and NABD (16-fold, Fig. 8) approximates the difference in cellular accumulation of each drug after a 2-h incubation (18-fold, Fig. 4). However, this relationship was not observed for the drug concentrations required for the inhibition of cellular macromolecular synthesis (Table 1). For example, there was a 67-fold difference in extra-cellular concentrations and a 5-fold difference in intracellular concentrations of the two drugs, associated with a 50% inhibition of [^{3}H]thymidine incorporation. Also, cells were exposed to each drug for 2 h, washed, and resuspended in fresh medium, and cell growth determined at 74 h. The short duration of drug exposure did not affect cell growth inhibition by DNR, whereas the NABD IC_{50} was highly dependent on the duration of exposure (Fig. 8).

Discussion

We have described the cellular pharmacodynamics of a new daunorubicin analogue, NABD, which has a photoactivatable *p*-azidobenzoyl group attached to the amino sugar. Following irradiation with ultraviolet light, this com-

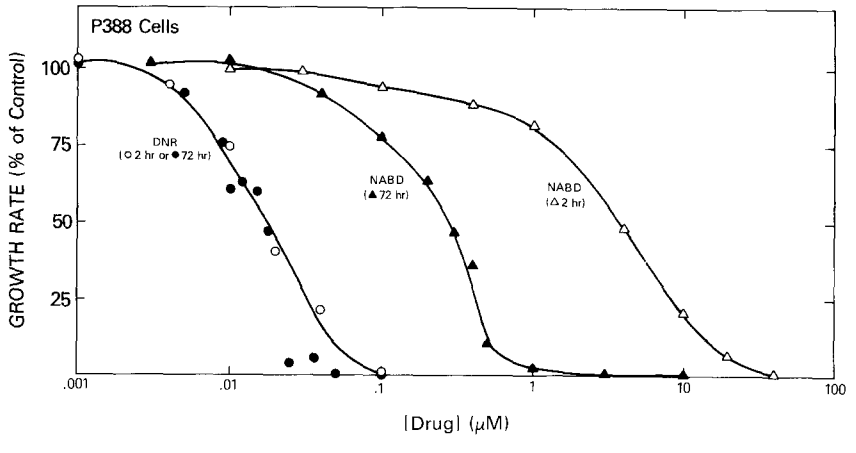

Fig. 8. Sensitivity of P388 cells to DNR and NABD. Cells (10^5/ml) were incubated for 2 h or 72 h with DNR or NABD. Cell density was determined at 72 h and growth rate calculated as described in *Materials and methods*. *Points* represent the means of triplicate samples from two to four separate experiments. Each SD was ≤16% of the mean

pound covalently binds specific cellular proteins in a variety of normal organs and cultured tumor cells in vitro [4, 5, 11, 18; R. L. Felsted et al., 1985, submitted for publication]. Whereas NABD shares structural similarities with its parent drug, the amino substitution results in significant changes in the biological and biochemical properties of NABD in tumor cells.

NABD was cytostatic against P388 cells in vitro, although significantly less potent than DNR (Fig. 8). The differences in antitumor activity may, in part, be explained by the different cellular pharmacological properties observed in this study. For instance, although NABD is very lipophilic, having a partition coefficient 70-fold larger than DNR, there was, nonetheless, significantly less cellular uptake of NABD. Although lipophilicity may determine cellular uptake characteristics of some anthracyclines [20], this is not always the case [13]; there may be additional mechanisms operative in the cellular accumulation of these drugs. For example, differences in drug pKa, high affinity for serum proteins present in the extracellular medium, less intracellular binding, and greater capacity for active cellular drug efflux may account for low cellular accumulation of NABD. In fact, additional experiments (not shown) demonstrate that the presence of FBS decreases cellular uptake of NABD 3-fold, whereas FBS has no effect on the cellular uptake of DRN [13]. Also, the lack of NABD nuclear cytofluorescence suggests that there may be fewer intracellular binding sites available for this drug, and that more NABD is therefore available for active extrusion by the cell. The rapid and apparent complete efflux of NABD from P388 cells occurs by a mechanism different from that of DNR, since the former process is only partially inhibited at 0 °C, in contrast to nearly complete inhibition of DRN efflux at 0 °C.

Presumably, one of the consequences of low intracellular accumulation of NABD is less effective inhibition of nucleic acid synthesis in growing tumor cells. In P388 cells grown in vitro, much greater extracellular concentrations of NABD than of DNR are required to inhibit radiolabeled thymidine incorporation by 50% (Table 1). However, higher intracellular NABD content is also required to achieve this level of inhibition, so that other mechanisms, e.g., less nuclear binding, in addition to drug transport may be operative. Alternatively, the inhibition of thymidine incorporation may be due to the effect of drug on nucleoside transport rather than direct interference with DNA synthesis [10]. In contrast, NABD inhibits RNA synthesis, as measured by radiolabeled uridine incorporation, more effectively than DNR does (Table 1). This selectivity against RNA synthesis is also found for other anthracyclines, including amino-substituted (e.g., *N*-trifluoroacetyl-adriamycin-14-valerate, *N,N*-dibenzyldaunorubicin and *N,N*-dimethyldaunorubicin) and class II (e.g., aclacinomycin and marcellomycin) analogues [1, 10, 12]. Furthermore, most of these compounds, as well as others of potential clinical importance, including *N*-acetyldaunorubicin, 4-demethoxydaunorubicin, and 7-con-*O*-methyl nogarol, demonstrate a predominant cytoplasmic localization when exposed to tumor cells in vitro [14]. In spite of this apparent cytoplasmic localization, these compounds are able to cause DNA damage [21] and inhibit nucleic acid synthesis [13, 14]. Thus, these drugs may act through mechanisms which differ from that of drugs such as DNR, which are located predominantly in the nucleus. Furthermore, these differences cannot be related simply to differences in total cellular accumulation of drug. Presumably these cytoplasmically localized analogues, including NABD, interact with non-nuclear cellular constituents and these interactions may mediate important biochemical events within the cell. For example, quinone-containing antibiotics may be activated in the cytoplasm by microsomal flavoproteins or mitochondrial enzymes to drug-free radicals. These radicals may then cause primary or secondary damage to nearby cellular components or they may travel into the nucleus to interact with DNA [7]. Further understanding of these interactions may be provided by photoaffinity labeling of NABD to tumor cells. For example, we have recently demonstrated that when NABD is incubated with P388 tumor cells and then photoactivated by UV light, there is specific covalent binding of the drug to a low-molecular-weight mitochondrial polypeptide. Furthermore, the photo labeling of this mitochondrial polypeptide with NABD is significantly enhanced in anthracycline-resistant P388 cells [5]. The function of this polypeptide and its role in anthracycline antibiotic mechanism of action is currently under investigation in our laboratory. Therefore, NABD appears to be useful as a mechanistic probe.

In summary, we have described the cellular pharmacology of NABD compared with that of DNR, and have shown that the photoaffinity analogue differs from that of its parent compound especially in its nuclear localization and its effect on nucleic acid synthesis. However, NABD retains antitumor activity in vitro and has properties similar to those of several active anthracycline analogues. Therefore, photoaffinity labeling studies utilizing NABD may identify important cytoplasmic macromolecules which interact with this type of anthracycline and perhaps with the anthracycline antibiotics in general to mediate biochemical events within the cell.

Acknowledgements. We wish to thank C. Glover, J. Sewell, and R. Bork for technical assitance and B. Sisco for assistance in preparing this manuscript.

References

1. Acton EM (1980) *N*-Alkylation of anthracyclines. In: Crooke ST, Reich SD (eds) Anthracyclines: Current status and new developments. Academic, New York, p 15
2. Andrews PA, Brenner DE, Chou FE, Kubo H, Bachur NR (1984) Facile and definitive determination of human adriamycin and daunorubicin metabolites by high-pressure liquid chromatography. Drug Metab Disp 8: 152
3. Arcamone F (1984) Antitumor anthracyclines: Recent developments. Med Res Rev 4: 153
4. Averbuch SD, Felsted RL (1984) Cellular pharmacology and protein binding of a photoactive anthracycline analogue. Proc Am Assoc Cancer Res 25: 295
5. Averbuch SD, Glover CJ, Sewell JL, Felsted RL (1985) Anthracycline photoaffinity labeling of an 18 kdalt protein in P388 sensitive and resistant cell lines. Proc Am Assoc Cancer Res 26: 223
6. Bachur NR, Gordon SL, Gee MV (1977) Anthracycline antibiotic augmentation of microsomal electron transport and free radical formation. Mol Pharmacol 13: 901
7. Bachur NR, Gee MV, Friedman RD (1982) Nuclear catalyzed antibiotic free radical formation. Cancer Res 42: 1078
8. Broggini M, Ghersa P, Donelli MG (1983) Subcellular distribution of adriamycin in the liver and tumor of 3LL-bearing mice. Eur J Cancer Clin Oncol 19: 419

9. Chowdry V, Westheimer FH (1979) Photoaffinity labeling of biological systems. Annu Rev Biochem 48: 293
10. Chuang RY, Chuang LF, Kawahata RT, Israel M (1983) Effect of *N*-trifluoroacetyladriamcin-14-valerate on [^{3}H]thymidine uptake and DNA synthesis of human lymphoma cells. J Biol Chem 258: 1062
11. Clawson RE, Felsted RL, Weiner M (1983) Characterization of an anthracycline binding protein from mouse liver. Proc Am Assoc Cancer Res 24: 254
12. Crooke ST, Duvernay VH, Mong S (1981) Molecular pharmacology of anthracyclines. In: Sartorelli AC, Lazo JS, Bertino JR (eds) Molecular actions and targets for cancer chemotherapeutic agents. Academic New York, p 137
13. Egorin MJ, Clawson RE, Ross LA, Bachur NR (1980) Cellular pharmacology of *N,N*-dimethyl daunorubicin and *N,N*-dimethyl adriamycin. Cancer Res 40: 1928
14. Egorin MJ, Clawson RE, Cohen JL, Ross LA, Bachur NR (1980) Cytofluorescence localization of anthracycline antibiotics. Cancer Res 40: 4669
15. Fedan JS, Hogaboom GK, O'Donnell JP (1984) Photoaffinity labels as pharmacological tools. Biochem Pharmacol 33: 1167
16. Felsted RL, Gee M, Bachur NR (1974) Rat liver daunorubicin reductase. An aldo-keto reductase. J Biol Chem 249: 3672
17. Felsted RK, Leavitt RD, Bachur NR (1975) Purification of phytohemaglutinin family of proteins from red kidney beans *(Phaseolus vulgaris)* by affinity chromatography. Biochim Biophys Acta 405: 72
18. Felsted RL, Glover CJ, Averbuch SD (1985) Rat heart anthracycline binding polypeptides (ABPs) identified by photoaffinity labeling. Proc Am Assoc Cancer Res 26: 7
19. Goormaghtigh E, Pollakis G, Ruysschaert JM (1983) Mitochondrial membrane modifications induced by adriamycin-mediated electron transport. Biochem Pharmacol 32: 889
20. Kessel D (1979) Biologic properties of three anthracyclines as a function of lipophilicity. Biochem Pharmacol 28: 3028
21. Krishan A, Dutt K, Israel M, Ganapathi R (1981) Comparative effects of adriamycin and *N*-trifluoroacetyladriamycin-14-valerate on cell kinetics, chromosomal damage, and macromolecular synthesis in vitro. Cancer Res 41: 2745
22. Londos-Gagliardi D, Capri M, Aubel-Sadron G, Maral R (1980) Subcellular localization of some anthracycline derivatives in Ehrlich ascites tumor cells. Biochem Biophys Res Commun 97: 397
23. Peterson C, Trouet A (1978) Transport and storage of daunorubicin and doxorubicin in cultured fibroblasts. Cancer Res 38: 4645
24. Sandberg JS, Howsden FL, DiMarco A, Goldin A (1970) Comparison of the antileukemic effect in mice of adriamycin (NSC 123127) with daunomycin (NSC 82151). Cancer Chemother Rep 54: 1
25. Siegfried JA, Kennedy KA, Sartorelli AC, Tritton TR (1983) The role of membranes in the mechanism of action of the antineoplastic agent adriamycin. J Biol Chem 258: 339
26. Smith TH, Fujiwara AN, Lee WW, Wu HY, Henry DW (1977) Synthetic approaches to adriamycin: 2. Degradation of daunorubicin to a nonasymmetric tetracyclic ketone and refunctionalization of the A ring to adriamycin. J Org Chem 42: 3653
27. Symposia (1975) Proceedings of the Fifth New Drug Seminar on Adriamycin, Washington, DC 16–17 December 1974 and the Adriamycin New Drug Seminar, San Francisco, 15–16 January 1975. Cancer Chemother Rep [3] 6: 83
28. Takanashi S, Bachur NR (1975) Daunorubicin metabolites in human urine. J Pharmacol Exp Ther 195: 41
29. Tsuruo T, Iida H, Kawabata H, Tsukagoshi S, Sakurai Y (1984) High calcium content of pleiotropic drug-resistant P388 and K562 leukemia and Chinese hamster ovary cells. Cancer Res 44: 5095
30. Zenebergh A, Baurain R, Trouet A (1982) Cellular pharmacokinetics of aclacinomycin A in cultured L1210 cells. Comparison with daunorubicin and doxorubicin. Cancer Chemother Pharmacol 8: 243

Received July 16, 1985/Accepted September 18, 1985